

A Distorted Trigonal Antiprismatic Cationic Silicon Complex with Ureato Ligands: Syntheses, Crystal Structures and Solid State ^{29}Si NMR Properties

Dana Schöne,^[a] Daniela Gerlach,^[a] Conny Wiltzsch,^[a] Erica Brendler,^[b] Thomas Heine,^[c] Edwin Kroke,^{*[a]} and Jörg Wagler^{*[a]}

Dedicated to Prof. Gerhard Roewer on the occasion of his 70th birthday

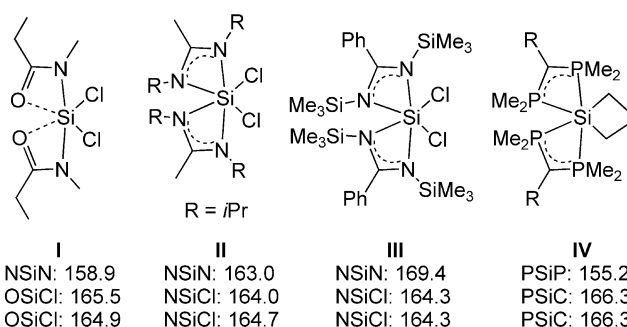
Keywords: Silicon / Chelates / Density-functional calculations / Hypercoordination

Insertion of phenyl isocyanate into the Si–N bond of *N*-(trimethylsilyl)diethylamine yields the *N'*-silylated *N,N*-diethyl-*N'*-phenylurea **1**, which undergoes transsilylation with SiCl_4 to yield the C_3 -symmetric cationic hexacoordinate silicon complex **3s⁺** [tris- κ -*O,N'*-(*N,N*-diethyl-*N'*-phenylureato)siliconium] as chloride salt, which was characterized crystallographically. The cationic complex **3s⁺** exhibits a distorted trigonal antiprismatic coordination sphere about the silicon atom with *fac* arrangement of the three N-atoms (and the three O-atoms) relative to one another. This C_3 -symmetric

complex undergoes isomerization into its asymmetric isomer **3a⁺** (*mer* arrangement of NNN or OOO relative to one another) in CDCl_3 solution. Hence, two ^{29}Si NMR signals appear and four sets of signals emerge in the ^1H and ^{13}C NMR spectra. Despite its pronounced axial symmetry, the ^{29}Si NMR shielding tensor of the cation **3s⁺** in its chloride salt exhibits an unusually small span (less than 20 ppm), which was analyzed CP/MAS NMR spectroscopically and by computational methods.

Introduction

Among the class of hypercoordinate silicon complexes^[1] those with a hexacoordinate silicon atom^[2] were found to exhibit more or less distorted octahedral coordination spheres. Deviation from the ideal octahedral geometry is mainly caused by different substituents X (thus resulting in different Si–X bond lengths) and steric strain, either caused by intramolecular sources such as chelate effects or by intermolecular interactions in the crystal packing. The most obvious sign for distortion of an octahedron is the deviation of the axial angles from 180° . As shown in Scheme 1 for selected examples of bis- and tris-chelate hexacoordinate silicon complexes^[3] the presence of small chelate rings results in pronounced distortion.



Scheme 1. Examples for “distorted octahedral” Si complexes. The three axial angles are given below the respective drawing. For **II** only data for one of the two crystallographically independent molecules are given here as representative example (for **IV**: R = PhMe_2Si).

The presence of different substituents in the octahedral coordination sphere of silicon was already shown to occasionally provoke a pronounced span of the ^{29}Si chemical shift anisotropy (CSA) tensor.^[2c,4] The transition to a more axial system, i.e., pentacoordinate silicon complexes with a trigonal bipyramidal Si-coordination sphere, causes an even wider span.^[5] To the best of our knowledge, the ^{29}Si NMR spectroscopic role of axial deformation of the octahedron with respect to the threefold axis, also creating a molecular system with a unique axis, has not been elucidated yet. Our recent investigations on silylated urea derivatives provided

[a] Institut für Anorganische Chemie, Technische Universität Bergakademie Freiberg, 09596 Freiberg, Germany
Fax: +49-3731-39-4058
E-mail: edwin.kroke@chemie.tu-freiberg.de
joerg.wagler@chemie.tu-freiberg.de

[b] Institut für Analytische Chemie, Technische Universität Bergakademie Freiberg, 09596 Freiberg, Germany

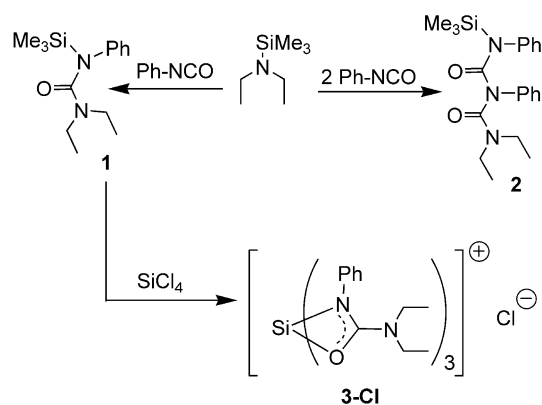
[c] School of Engineering and Science, Theoretical Physics – Theoretical Materials Science, Jacobs University Bremen, 28759 Bremen, Germany

Supporting information for this article is available on the WWW under <http://dx.doi.org/10.1002/ejic.200900784>.

access to a cationic hexacoordinate siliconium complex comprising three four-membered chelate rings, resulting in a pronounced C_3 -symmetric deformation of the coordination sphere from octahedral towards distorted antiprismatic. Thus, this interesting complex was subjected to X-ray diffractational, ^{29}Si NMR spectroscopic and computational analyses.

Results and Discussion

Phenyl isocyanate reacts with *N*-(trimethylsilyl)diethylamine under formal insertion into the Si–N bond, thus providing convenient access to the *N'*-trimethylsilylated *N,N*-diethyl-*N'*-phenylurea **1**, whereas excess of phenyl isocyanate would lead to the formation of **2** as a by-product (Scheme 2). Synthesis of **1** in hexane, however, provides a product of sufficient purity for further reactions since **1** is obtained as a hexane-soluble colorless oil, whereas compound **2**, even though formed as a minor by-product, precipitates from hexane to yield white crystalline needles suitable for X-ray diffraction analysis (Figure 1).



Scheme 2. Synthesis of the silylated urea derivative **1** and the hexacoordinate silicon compound **3-Cl** thereof (representation of one canonical form).

Deliberate synthesis of **2** by treating *N*-(trimethylsilyl)diethylamine with two equivalents of phenyl isocyanate proved a convenient route to generate this interesting ligand precursor in reasonable yield. In the present work, however, we want to focus on **1** as a chelating ligand precursor.

As shown in previous reports, trimethylsilylated (*O,N*)-chelators proved useful as starting materials in the syntheses of hypercoordinate silicon chelate complexes since the by-product of the reactions, Me_3SiCl , is volatile and may be easily removed from the product.^[1a,1b] So far, a number of carboxylic acid derivatives such as carboxylates,^[6] amides^[3a] and amidinates^[3b,3c] has been studied as ligands capable of setting up coordination spheres with coordination number 5 or 6 about a silicon atom. Whereas the former were occasionally found to act as bidentate chelators, urea moieties, although reported in the context of silicon coordination chemistry, served the role of a monodentate donor or were bidentately bound to the Si-atom in a $\kappa(\text{O,C})$ -mode.^[7]

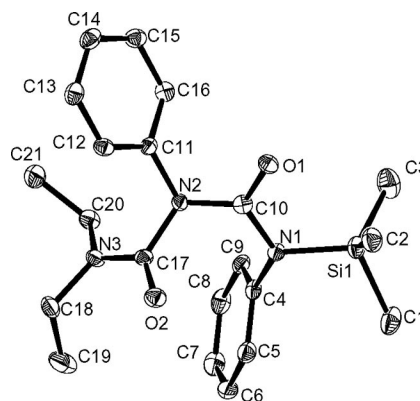
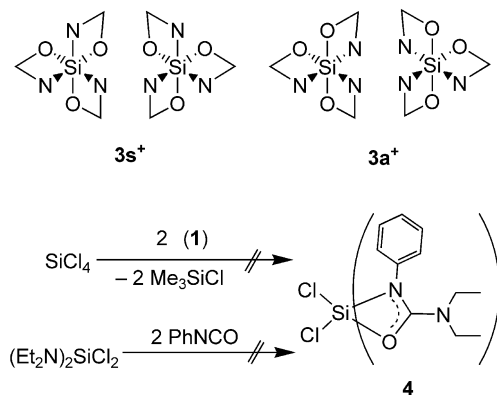


Figure 1. ORTEP drawing of **2** in the crystal (ellipsoids at the 50% probability level, hydrogen atoms omitted for clarity). Selected bond lengths [Å] and dihedral angles [°]: Si1–N1 1.783(2), O1–C10 1.225(2), O2–C17 1.222(2), N1–C10 1.374(3), N2–C10 1.401(2), N2–C17 1.437(3), N3–C17 1.354(2), Si1–N1–C10–N2 177.3(1), N1–C10–N2–C17 41.9(3), C10–N2–C17–N3 149.0(2), N2–C17–N3–C18 169.2(2).

Hence, we probed the chelator qualities of compound **1** in a reaction with silicon tetrachloride (Scheme 2, bottom). The reaction proceeds towards the cationic tris-chelate **3⁺** (which was found to exist in two diastereomeric forms in solution, i.e., the enantiomers of the asymmetric **3a⁺** and the C_3 -symmetric **3s⁺** cations) in a clean manner. In the ^{29}Si solid state NMR spectrum only one signal was detected at $\delta = -165.9$ ppm. Attempts to synthesize the bis-chelate complex **4** by adjusting the molar ratio $1/\text{SiCl}_4$ to 2:1 failed: The co-existence of **3⁺** and unreacted SiCl_4 was proven ^{29}Si NMR spectroscopically. Apparently, the mono- and di-substituted silanes LSiCl_3 and L_2SiCl_2 , respectively, ($\text{L} = \text{N,N}$ -diethyl-*N'*-phenylureate) exhibit enhanced reactivity relative to SiCl_4 , thus furnishing **3⁺** as the final substitution product. In order to explore an alternative route towards compound **4** phenyl isocyanate was treated with bis(diethylamino)dichlorosilane. Again, complex **3⁺** was formed, thus hinting at ligand scrambling which should have given rise to the formation of **3⁺** from intermediately formed **4** (not detected; Scheme 3).



Scheme 3. Top: schematic representation of the two pairs of diastereomers of the cation **3⁺** found in chloroform solution (**3s⁺** = *fac*, **3a⁺** = *mer*). Bottom: attempts to synthesize **4**, leading also to **3-Cl**.

In addition to not delivering the desired product **4**, this alternative route resulted in the formation of a byproduct, namely trimerized phenyl isocyanate, which crystallizes with **3s-Cl** as **3s-Cl·THF·(PhNCO)₃** (**structure A**) (Figure 2). From the same reaction further crystals were obtained which consist of **3s-Cl** only (**structure B**) (Figure 3). The presence of more than one hexacoordinate silicon compound in the solid obtained was furthermore indicated by ²⁹Si CP/MAS NMR spectra, which produced a peak at $\delta = -165.9$ ppm (as for the former product) and a less intense one at $\delta = -164.1$ ppm (with a shoulder). Except the special features caused by the additional components in the crystal structure [interaction between chloride and (PhNCO)₃ with a separation of 3.028(1) Å between Cl⁻ and the centroid of the triazine system, as well as a THF molecule located on a threefold axis with its O-atom pointing towards the Si-atom of **3s⁺** from a distance of 5.522(3) Å] the features of the cation **3s⁺** are very similar in both solids (see Figure caption 3). Thus, only the molecular structure of **3s-Cl** will be discussed. As indicated in the canonical formula in Scheme 2, bottom, and by the bond lengths C7–N1 and C7–N2, the diethylamino substituent donates electron density towards the ligand donor sites, thus enhancing the double bond character of bond C7–N2, whereas bonds C7–O1 and C7–N1 represent single bonds strengthened by π -conjugation. This additional donor action of N2 can be considered source of the structural differences between the ureato ligand in **3s⁺** and the carbamido ligand in the complex Scheme 1 **I**,^[3a] which exhibits shorter C–O and C–N bonds (1.299, 1.308 and 1.300, 1.303 Å, respectively). In a related study, Kost et al. have shown that the transition from hydrazinimides to semicarbazones is also accompanied by reinforcement of the ligand donor capabilities by the additional R₂N group,^[8] and the same was shown to apply to pyridine ligands upon substitution with a 4-dimethylamino group.^[4a] Hence, the ureato ligand in **3s⁺** is setting up Si–N and Si–O bonds of similar length, whereas in the carbamide complex **A** in Scheme 1 the Si–O bonds (1.885, 1.886 Å) are longer than the Si–N bonds (1.830, 1.835 Å), again accounting for the carbamide character of the ligand utilized by Yang and Verkade. In addition to the axial angles being much smaller than 180°, the coordination sphere about the silicon atom in **3s⁺** deviates from octahedral by two distinct features: These are (i) the significantly reduced rotation of the two opposite triangular faces NNN and OOO by only 40.7(1)°, which corresponds to a 32.2% rotation towards trigonal prismatic, and (ii), the noticeably low ratio [IPD/AEL_(complex)] = 0.666 (IPD = inter-planar distance, AEL = average edge length of the triangles, [IPD/AEL_(octahedron)] = 0.816), thus confirming 18.4% compression of the octahedron along the ideal threefold axis. Thus, one cannot consider this coordination geometry as slightly distorted octahedral any longer, whereas distorted trigonal antiprismatic would hold for any rotation angle between 30 and 60° regardless the degree of compression or stretching of the two parallel triangular faces along the threefold axis.

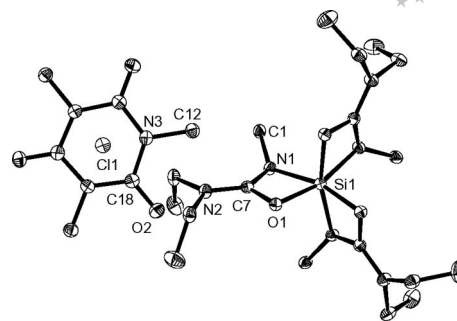


Figure 2. ORTEP drawing of **3s⁺** and the (PhNCO)₃·Cl⁻ counterion in the crystal structure of **3s-Cl·THF·(PhNCO)₃** (**structure A**) (view along the crystallographic *c*-axis, 30% probability ellipsoids, hydrogen atoms, THF molecule and phenyl groups omitted, selected atoms of asymmetric unit labeled). Atoms Si1 and Cl1 are located on threefold axes.

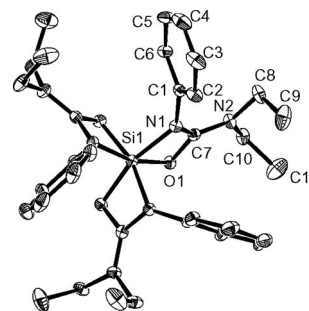


Figure 3. ORTEP drawing of **3s⁺** in the crystal structure of **3s-Cl** (**structure B**) (30% probability ellipsoids, hydrogen atoms omitted, atoms of asymmetric unit labeled). Selected bond lengths [Å] and angles [°] of **3s⁺** in **3s-Cl**: Si1–O1 1.810(2), Si1–N1 1.833(2), O1–C7 1.323(3), N1–C7 1.344(3), N2–C7 1.318(3), O1–Si1–N1 71.8(1), C7–N2–C8 121.7(2), C7–N2–C10 119.9(2), C8–N2–C10 118.2(2); corresponding parameters of **3s⁺** in **3s-Cl·THF·(PhNCO)₃**: Si1–O1 1.800(1), Si1–N1 1.840(2), O1–C7 1.315(2), N1–C7 1.346(2), N2–C7 1.315(2), O1–Si1–N1 71.9(1), C7–N2–C8 121.3(2), C7–N2–C10 119.4(2), C8–N2–C10 119.0(1).

Although the axial angles N–Si–O* [162.8(1)°] are in the same range as the inter-chelate axial angles of the compounds depicted in Scheme 1 (in **3s-Cl** position O* is generated from O1 by operation $2 - y, 1 + x - y, z$), the three identical chelates create a particularly high symmetry of this tris-chelate complex. The pronounced C₃-symmetric distortion of the Si-coordination sphere in **3s⁺**, which should result in pronounced axiality of the ²⁹Si NMR CSA tensor, tempted us to analyze this property experimentally and computationally. Since the product obtained from the reaction of phenyl isocyanate with bis(diethylamino)dichlorosilane was contaminated with by-products, the compound obtained from the reaction of **1** with SiCl₄ was used for ²⁹Si CP/MAS NMR analysis of the CSA tensor. The ²⁹Si CP/MAS NMR spectrum of **3s-Cl**, depicted in Figure 4, reveals a very narrow span of the chemical shift anisotropy. Although the axiality of the CSA tensor can be discerned from the principal component δ_{22} being closer to δ_{33} than to δ_{11} , this result was not expected.

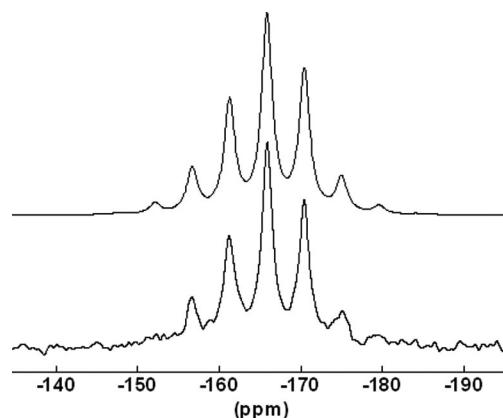


Figure 4. Bottom: ^{29}Si CP/MAS NMR spectrum of **3s-Cl** ($v_{\text{spin}} = 364$ Hz). Top: overlay of the simulated spectrum using the CSA tensor data from the entry “exp.” in Table 1.

We analyzed the CSA tensor by means of quantum chemistry, approximating the solid-state structure by the formally positively charged cation 3s^+ at the frozen low-temperature XRD **structure B**. The CSA tensor, computed at various DFT and HF levels, confirms the narrow span (Table 1). The skew, which must be -1 in this axial molecular system according to the system's C_3 symmetry (two degenerate principal axes in the molecular and crystal environment of threefold symmetry), was not reproduced as such by the experimental methods applied. HF and DFT approaches with larger basis sets (i.e. calculations 4 and 5) converge to similar results, which indicates that theory can describe the model compound rather well, as both methods contain quite different approximations. In conclusion, all methods applied proved suitable to describe the narrow span of the CSA tensor, which is located in the cation as follows: Component (11) points along the threefold axis, whereas components (22) and (33) are degenerate in the plane orthogonal to the threefold axis.

Table 1. ^{29}Si NMR CSA tensor of 3s^+ determined experimentally and computationally for **structure B**. The principal components δ_{11} , δ_{22} and δ_{33} as well as the span Ω and skew κ are given according to the Herzfeld–Berger notation.^[9]

Entry ^[a]	δ_{iso}	δ_{11}	δ_{22}	δ_{33}	Ω	κ
exp.	-165.9	-154.7	-167.1	-175.8	21.1	-0.17
calc1	-176.2	-168.1	-180.3	-180.3	12.2	-1.00
calc2	-170.1	-162.2	-174.1	-174.1	11.9	-1.00
calc3	-165.2	-155.3	-170.2	-170.2	14.9	-1.00
calc4	-173.3	-163.4	-178.3	-178.3	14.9	-1.00
calc5	-171.9	-164.4	-175.7	-175.7	11.3	-1.00

[a] Exp.: determined from the MAS spectrum at $v_{\text{spin}} = 364$ Hz, calc1: DFT-IGLO-III (PBE), calc2: B3LYP/6-311G(d,p), calc3: HF/6-311G(d,p), calc4: HF/6-311G(2d,p), calc5: GIAO-PBE/TZ2P (Slater basis).^[10]

Analysis of the contributions to the overall shielding with DFT-IGLO (using Pipek–Mezey localization) confirmed similar influence of the oxygen and nitrogen donor atoms, as shown in Table 2. Whereas one dominating lone pair contribution was analyzed for the N-atoms (e.g., N -47.9), the oxygen atoms were found to exhibit two distinct lone

pair contributions (e.g., O -14.9 and -25.3), the sum of which, however, is close to the N-atom influence. Due to the C_3 symmetry of the cation, the influences of all O-atoms (the same holds for the N-atoms) in direction (11) is equal, whereas the degenerate character of (22) and (33) is reflected in the permutational influence of the O- and N-atoms in these directions.

Table 2. Selected individual contributions to the ^{29}Si shielding tensor of 3s^+ , determined using DFT-IGLO-III (Pipek–Mezey localization).

Atom ^[a]	σ_{iso}	σ_{11}	σ_{22}	σ_{33}
O	-14.9	-14.8	-4.3	-25.7
O	-25.3	-22.4	-12.7	-40.6
O*	-15.0	-14.8	-18.5	-11.8
O*	-25.2	-22.5	-43.4	-9.9
O**	-14.9	-14.8	-22.4	-7.6
O**	-25.3	-22.6	-23.8	-29.5
N	-47.9	-51.6	-52.6	-39.4
N*	-48.0	-51.7	-14.0	-78.4
N**	-48.0	-51.5	-71.9	-20.5

[a] The asterisked atoms represent symmetry equivalents in the crystal system.

So far, no satisfactory explanation was found for the skew of the CSA tensor deviating from -1 in the experiment. Thermal motion of the molecules in the crystal at elevated temperatures was considered to violate the perfect C_3 symmetry, hence influencing the shape of the CSA tensor. In order to probe this hypothesis, the collection of an X-ray diffraction data set at elevated temperatures was planned, and a tiny single-crystalline needle (from the sample which was used for CSA tensor analysis) was chosen for data collection. Unit cell determination at 250 K revealed trigonal cell parameters, but different from those of compound **3s-Cl**, the structure of which was determined at 150 K ($a = 20.109$, $c = 14.518$ Å for the former, $a = 12.028$, $c = 14.354$ Å for the latter). Upon cooling to 150 K and further to 100 K no phase transition (at least by means of striking changes in the unit cell parameters) was observed. Structure solution revealed a further trigonal modification of **3s-Cl** (**structure C**, space group $P3$), but with six crystallographically independent Si-environments. The molecular shapes of the six individual cations 3s^+ are similar to those in **structure B** (space group $P31c$), thus rendering further discussion of bond lengths and angles superfluous. **Structure C** (at 100 K) exhibits an average molecular volume of 847 Å³ per unit **3s-Cl**. In sharp contrast, the spatial demand of **3s-Cl** in **structure B** (at 150 K) is much greater with 899 Å³. This notable difference, which does not only originate from the different temperatures of X-ray data collection, gives rise to the assumption that the more closely packed **structure C** should be the more stable one (rendering the crystal of **structure B** a discovery by chance). Indeed, repeated crystal picking and unit cell determination of crystals obtained from the reaction of bis(diethylamino)dichlorosilane and phenyl isocyanate (upon storage of the reaction mixture for 3 weeks) revealed that, in addition to **3s-Cl-THF·(PhNCO)₃** (**structure A**), crystals of **3s-Cl** (**structure C**) were present in the solid product.

Despite similar Si–N and Si–O bond lengths, the trigonal-antiprismatic distortion of the six individual Si-coordination spheres in **structure C** varies slightly (with the distortion towards trigonal-prismatic ranging from 32.3 to 36.3%, the compression along the threefold axis ranging from 15.7 to 16.9%). Characteristic parameters of the Si-coordination polyhedra in **structure C** are summarized in Table 3.

Table 3. Geometric parameters of the Si-coordination spheres of the six individual cations 1–6 in the crystal **structure C** of **3s-Cl**. [edge lengths N···N' and O···O', the average edge length (AEL) thereof and NNN-OOO inter-planar distance (IPD) of the trigonal-antiprisms in Å, dihedral angle of the O- and N-donor atom of one chelate about the C₃-axis (tors.(O–C₃–N)) in °].

Cation	1	2	3	4	5	6
$d(\text{N}\cdots\text{N}')^{[a]}$	2.795	2.795	2.801	2.800	2.807	2.779
$d(\text{O}\cdots\text{O}')^{[a]}$	2.642	2.626	2.621	2.634	2.611	2.641
tors. (O–C ₃ –N) ^[b]	40.04	39.97	38.94	40.62	38.20	40.01
% trig. prism.	33.3	33.4	35.1	32.3	36.3	33.3
AEL	2.7185	2.7105	2.711	2.717	2.709	2.710
IPD	1.853	1.852	1.865	1.843	1.863	1.858
IPD/AEL	0.682	0.683	0.688	0.678	0.688	0.686
% compression	16.4	16.3	15.7	16.9	15.7	15.9

[a] Standard deviation: 0.004. [b] Standard deviation: 0.15.

These six slightly different coordination spheres might give rise to six CSA tensors of slightly different span, the superposition of which would provide an explanation for the ²⁹Si solid state NMR spectrum observed in the experiment (Figure 4). In order to get an idea of the variability of the span of the CSA tensor among these six cations their solid-state structures were, upon optimization of the H-positions, employed for CSA tensor calculation on the HF/6-311G(d,p) level. The results, listed in Table 4, indeed offer an explanation for seemingly lower axiality of the CSA tensor observed in the experiment. Although the isotropic chemical shift was predicted to be very similar for the six independent ²⁹Si nuclei, the CSA tensors of cations 3 and 5 (which exhibit pronounced distortion of the coordination sphere towards trigonal prismatic) can be expected to show a larger span than the other four cations. Upon removal of the computational error on the value of δ_{iso} (i.e., upon setting $\delta_{\text{iso}} = -165.9$ ppm for each of the six CSA tensors in Table 4), the superposition of the six individual spectra created therefrom (each of the six individual Si nuclei contributing with 16.7%) indeed produces a picture which reflects the experimental data very well (Figure 5). Although a plausible explanation was found, additional effects of mo-

Table 4. ²⁹Si NMR CSA tensor of **3s⁺** for the six independent cations of **structure C**, determined computationally using HF/6-311G(d,p). The principal components δ_{11} , δ_{22} and δ_{33} as well as the span Ω are given according to the Herzfeld–Berger notation.^[9]

Cation	1	2	3	4	5	6
δ_{iso}	-162.1	-163.3	-162.8	-162.9	-162.7	-164.7
δ_{11}	-152.4	-153.1	-150.9	-154.2	-148.8	-154.2
δ_{22}	-166.7	-168.3	-168.8	-166.9	-169.7	-169.9
δ_{33}	-167.2	-168.3	-168.8	-166.9	-169.7	-169.9
Ω	14.8	15.2	17.9	12.8	20.9	15.7

lecular thermal motion at room temperature might also contribute to the overall shape of the experimental ²⁹Si CP/MAS NMR spectrum of **3s-Cl** (**structure C**).

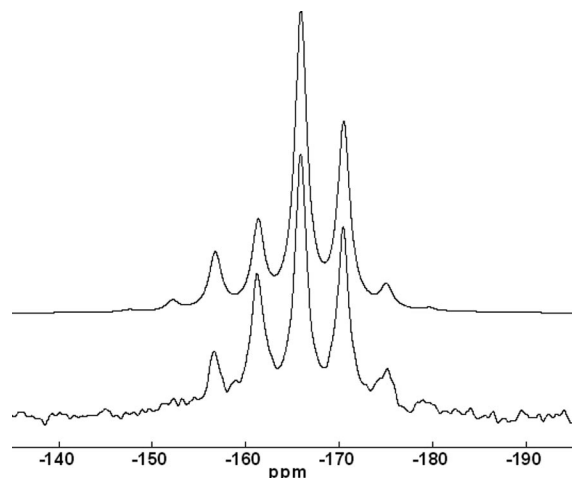


Figure 5. Bottom: ²⁹Si CP/MAS NMR spectrum of **3s-Cl** ($\nu_{\text{spin}} = 364$ Hz). Top: simulated spectrum using the weighted CSA tensor data (16.7% contribution of each tensor) from Table 4 (upon setting $\delta_{\text{iso}} = -165.9$ ppm for each of the six CSA tensors).

Conclusions

The insertion of phenyl isocyanate into the Si–N bond of a trimethylsilylamine was shown to provide convenient access to an interesting class of chelating ureato systems, the coordination behavior of which will be addressed in further studies. A first example of a hexacoordinate silicon complex synthesized therefrom already revealed some special features of these ligands in exhibiting donor qualities different from those of related carbamide systems (**I**, Scheme 1): the electron releasing diethylamino substituent supports strong coordination of both the N- and O-donor site. This pronounced stabilizing effect of the (O,N) chelate is considered to facilitate the formation of the herein presented silicon tris-chelate **3⁺** (in sharp contrast to the bis-chelates **I**, **II** and **III** in Scheme 1). The special coordination geometry of this silicon complex, i.e., distorted trigonal antiprismatic, was found to give rise to a very narrow ²⁹Si NMR shielding tensor. The pronounced axiality of the Si-coordination sphere (C₃ symmetry) was expected to generate a ²⁹Si solid state NMR spectrum also exhibiting pronounced axiality. Instead, a less axial CSA tensor was found in the experiment, hinting at effects like disturbances of the ideal C₃ symmetry in the crystal lattice at ambient temperatures and at the superposition of various axial CSA tensors of different span. Whereas the symmetry-disturbing influence of molecular thermal motion at room temperature can always be considered a source of error, repeated single crystal structure analyses proved the latter hypothesis true and ²⁹Si solid state NMR spectroscopy a valuable tool complementing X-ray diffraction analyses.

Experimental Section

Synthesis of *N,N*-Diethyl-*N'*-(trimethylsilyl)-*N'*-phenylurea (1**):** To a solution of *N*-(trimethylsilyl)diethylamine (10.8 g, 74.4 mmol) in hexane (50 mL), which was stirred in a 15 °C water bath, phenyl isocyanate (9.32 g, 78.3 mmol) was added dropwise within a few minutes and stirring was continued for 3 h. Within this time some white crystalline precipitate formed (1.38 g, 3.6 mmol, 4.8% of **2**, as identified later), which was filtered off. Upon removal of the volatiles from the filtrate under reduced pressure product **1** remains in the flask as a viscous yellowish oil. NMR spectroscopy indicated sufficient purity for further reactions. (Yield: 18.6 g, 70.5 mmol, 95%). NMR spectra of **1** exhibit broadened signals originating from configurational exchange processes at the urea moiety. ¹H NMR (400.13 MHz, CDCl₃, 22 °C): δ = 0.2 [br. s, 9 H, Si(CH₃)₃], 0.84 (br. s, 6 H, NCH₂CH₃), 3.11 (br. s, 4 H, CH₂), 6.9–7.3 (3m, 4 H, 2 H, 4 H, Ph) ppm. ¹³C NMR (100.62 MHz, CDCl₃, 22 °C): δ = -0.1 [-Si(CH₃)₃], 12.2 (NCH₂CH₃), 41.5 (CH₂), 124.2, 127.0, 128.4, 143.4 (Ph), 162.5 (C=O) ppm. ²⁹Si NMR (79.5 MHz, CDCl₃, 22 °C): δ = 8.5 ppm (br.).

This compound is very sensitive towards hydrolysis. Although stored in a sealed Schlenk flask, some crystals of the *N,N*-diethyl-*N'*-phenylurea, obviously liberated by traces of moisture, formed upon storage of the remaining product for some weeks. The solid-state structure of *N,N*-diethyl-*N'*-phenylurea was confirmed X-ray crystallographically. CCDC-743688, crystal dimensions 0.40 × 0.12 × 0.04 mm, C₁₁H₁₆N₂O, *M_r* = 192.26, *T* = 90(2) K, orthorhombic, space group *Pbcn*, *a* = 15.1284(8), *b* = 8.8584(4), *c* = 16.3355(8) Å, *V* = 2189.18(19) Å³, *Z* = 8, ρ_{calcd.} = 1.167 Mg m⁻³, μ(Mo-*K_α*) = 0.076 mm⁻¹, *F*(000) = 832, 2θ_{max} = 52.0°, 16958 collected reflections, 2139 unique reflections (*R*_{int} = 0.0654), 132 parameters, *S* = 1.004, *R*₁ = 0.0391 [*I* > 2σ(*I*)], *wR*₂(all data) = 0.0951, max./min. residual electron density +0.188/-0.225 e Å⁻³.

Synthesis of Compound 2: To a solution of *N*-(trimethylsilyl)diethylamine (3.79 g, 26.1 mmol) in hexane (50 mL), which was stirred in a 15 °C water bath, phenyl isocyanate (6.21 g, 52.2 mmol) was added dropwise within a few minutes and stirring was continued for further 15 min. Within this time precipitation of **2** commenced. The mixture was stored at room temperature overnight, whereupon the solid product was filtered off, washed with hexane (20 mL) and dried in vacuo; yield 7.96 g, 20.8 mmol, 79.7%; m.p. 112 °C. C₂₁H₂₉N₃O₂Si (383.56): calcd. C 65.76, H 7.62, N 10.96; found C 66.19, H 7.26, N 10.99. ¹H NMR (400.13 MHz, CDCl₃, 22 °C): δ = 0.21 [s, 9 H, Si(CH₃)₃], 0.54 (br. s, 6 H, NCH₂CH₃), 2.72 (br. s, 4 H, CH₂), 6.9–7.3 (3m, 4 H, 2 H, 4 H, Ph) ppm. ¹³C NMR (100.62 MHz, CDCl₃, 22 °C): δ = -0.1 [-Si(CH₃)₃], 11.7 (NCH₂CH₃), 41.3 (CH₂), 125.8, 126.0, 126.1, 128.3, 129.0, 129.6, 140.6, 141.1 (Ph), 156.3, 161.3 (C=O) ppm. ²⁹Si NMR (79.5 MHz, CDCl₃, 22 °C): δ = 12.4 ppm. X-ray structure analysis of **2**. CCDC-743689, crystal dimensions 0.30 × 0.10 × 0.03 mm, C₂₁H₂₉N₃O₂Si, *M_r* = 383.56, *T* = 100(2) K, monoclinic, space group *P2₁/c*, *a* = 17.3226(7), *b* = 6.3823(2), *c* = 20.2088(7) Å, β = 111.396(2)°, *V* = 2080.26(13) Å³, *Z* = 4, ρ_{calcd.} = 1.225 Mg m⁻³, μ(Mo-*K_α*) = 0.133 mm⁻¹, *F*(000) = 824, 2θ_{max} = 50.0°, 13391 collected reflections, 3668 unique reflections (*R*_{int} = 0.0563), 249 parameters, *S* = 0.963, *R*₁ = 0.0426 [*I* > 2σ(*I*)], *wR*₂(all data) = 0.0925, max./min. residual electron density +0.263/-0.265 e Å⁻³.

Synthesis of Tris-κ-O,*N'*-(*N,N*-diethyl-*N'*-phenylureato)siliconium Chloride (3-Cl**):** To a solution of **1** (17.8 g, 67.4 mmol) in chloroform (30 mL), which was stirred in a 15 °C water bath, SiCl₄ (3.82 g, 22.5 mmol) was added dropwise within a few minutes and stirring was continued for further 2 h. The color of the solution slowly changed from colorless via yellow to brownish-red. The vol-

atiles were removed under reduced pressure and the remaining viscous oil was dissolved in THF (50 mL), whereupon crystallization of **3s-Cl** commenced overnight. After 24 h the solid was filtered off, washed with THF (3 × 5 mL) and dried in a vacuum. (Yield: 3.33 g, 5.23 mmol, 23%). This compound decomposes without melting when heated up to 300 °C in a sealed capillary. C₃₃H₄₅ClN₆O₃Si (637.29): calcd. C 62.20, H 7.12, N 13.19; found C 61.85, H 7.11, N 12.99. The NMR spectra of a solution of **3-Cl** in CDCl₃ exhibit sets of signals corresponding to a mixture of the isomeric cations **3s⁺** and **3a⁺** in solution. The ¹H NMR spectrum exhibits various superimposed triplets in the range 0.6–1.4 ppm originating from the ethyl-CH₃ groups and quartets in the range 2.8–3.6 ppm for the CH₂ groups. Even less informative is the part of the aromatic proton signals. The ¹³C NMR spectroscopic data, however, clearly show the presence of 3 small signals of equal intensity for **3a⁺** and, in the same chemical shift range, one intense signal for **3s⁺** in distinct parts of the spectrum, whereas the chemical shift range of the phenyl-*o,m,p*-carbon atoms is characterized by various superimposed signals (125.0, 125.7, 126.3, 126.6, 127.0, 127.8, 128.4, 129.2, 129.4, 129.7 ppm). For clarity reasons selected ¹³C NMR spectroscopic data are presented in Table 5.

Table 5. ¹³C NMR spectroscopic data of **3-Cl** (chemical shift δ in ppm) in CDCl₃ solution at 22 °C.

δ for 3s⁺	δ for 3a⁺	Moiety
12.8, 13.7	12.6, 12.9 (2×), 13.1, 13.4, 14.0	CH ₃
41.4, 44.1	41.3, 41.6, 42.1, 43.5, 44.1 (2×)	CH ₂
137.7	137.1, 137.5, 138.2	Ph- <i>ipso</i>
160.2	159.6, 159.7, 160.8	C=O

²⁹Si NMR (79.5 MHz, CDCl₃, 22 °C): δ = -168.2, -169.7 ppm, similar intensity. ²⁹Si NMR (79.5 MHz, solid state, CP, ν_{spin} = 4 kHz): δ_{iso} = -165.9 ppm.

X-ray Crystal Structure Analysis of 3s-Cl (structure C): CCDC-743692, crystal dimensions 0.38 × 0.12 × 0.08 mm, C₃₃H₄₅ClN₆O₃Si, *M_r* = 637.29, *T* = 100(2) K, trigonal, space group *P3*, *a* = *b* = 20.1088(3), *c* = 14.5184(5) Å, *V* = 5084.2(2) Å³, *Z* = 6, ρ_{calcd.} = 1.249 Mg m⁻³, μ(Mo-*K_α*) = 0.190 mm⁻¹, *F*(000) = 2040, 2θ_{max} = 50.0°, 33245 collected reflections, 10598 unique reflections (*R*_{int} = 0.0665), 793 parameters, *S* = 0.993, Flack parameter -0.03(5), *R*₁ = 0.0493 [*I* > 2σ(*I*)], *wR*₂(all data) = 0.0966, max./min. residual electron density +0.448/-0.302 e Å⁻³.

In an alternative attempt, **3s-Cl** was obtained from the reaction of bis(diethylamino)dichlorosilane with phenyl isocyanate: To a solution of bis(diethylamino)dichlorosilane (2.50 g, 10.3 mmol) in THF (20 mL) phenyl isocyanate (2.45 g, 20.6 mmol) was added dropwise. From the clear solution white crystals formed within one day upon storage at room temperature. The supernatant was decanted and the crystals were briefly dried in vacuo. Yield: 1.13 g. This product, however, consisted of various crystalline compounds as recognized by ²⁹Si solid state NMR spectroscopy (CP/MAS, ν_{spin} = 4 kHz), signals at δ_{iso} = -165.9, -164.1 ppm, two of which were identified crystallographically as **3s-Cl·THF·(PhNCO)₃** (structure A) and **3s-Cl** (structure B).

X-ray Crystal Structure Analysis of 3s-Cl·THF·(PhNCO)₃ (structure A): CCDC-743690, crystal dimensions 0.35 × 0.30 × 0.25 mm, C₅₈H₆₈ClN₉O₇Si, *M_r* = 1066.75, *T* = 150(2) K, trigonal, space group *R3c*, *a* = *b* = 11.8203(1), *c* = 70.3118(14) Å, *V* = 8507.8(2) Å³, *Z* = 6, ρ_{calcd.} = 1.249 Mg m⁻³, μ(Mo-*K_α*) = 0.148 mm⁻¹, *F*(000) = 3396, 2θ_{max} = 52.0°, 21647 collected reflections, 3623 unique reflections (*R*_{int} = 0.0293), 237 parameters, *S* = 1.067, Flack parameter 0.03(7), *R*₁ = 0.0322 [*I* > 2σ(*I*)], *wR*₂(all

data) = 0.0784, max./min. residual electron density +0.288/−0.238 eÅ^{−3}.

X-ray Crystal Structure Analysis of 3s-Cl (structure B): CCDC-743691, crystal dimensions 0.45 × 0.30 × 0.25 mm, C₃₃H₄₅ClN₆O₃Si, *M_r* = 637.29, *T* = 150(2) K, trigonal, space group *P*31*c*, *a* = *b* = 12.0280(6), *c* = 14.3543(14) Å, *V* = 1798.5(2) Å³, *Z* = 2, $\rho_{\text{calcd.}}$ = 1.177 Mg m^{−3}, $\mu(\text{Mo-K}\alpha)$ = 0.179 mm^{−1}, *F*(000) = 680, $2\theta_{\text{max}}$ = 50.0°, 6127 collected reflections, 2109 unique reflections (*R_{int}* = 0.0402), 135 parameters, *S* = 1.023, Flack parameter 0.00(10), *R*₁ = 0.0371 [*I* > 2σ(*I*)], *wR*₂(all data) = 0.0852, max./min. residual electron density +0.167/−0.180 eÅ^{−3}.

Supporting Information (see also the footnote on the first page of this article): Color representations of the six independent cations 3s⁺ of structure C of 3s-Cl.

Acknowledgments

TU Bergakademie Freiberg and the Deutsche Forschungsgemeinschaft (DFG) are acknowledged for financial support of this work.

- [1] Selected reviews on hypercoordinate silicon chemistry: a) D. Kost, I. Kalikhman, *Acc. Chem. Res.* **2009**, *42*, 303–314; b) D. Kost, I. Kalikhman, *Adv. Organomet. Chem.* **2004**, *50*, 1–106; c) R. Tacke, M. Pülm, B. Wagner, *Adv. Organomet. Chem.* **1999**, *44*, 221–273; d) C. Chuit, R. J. P. Corriu, C. Reye, J. C. Young, *Chem. Rev.* **1993**, *93*, 1371–1448; e) R. J. P. Corriu, C. Guerin, J. J. E. Moreau, in: *Chem. Org. Silicon Compd.* (Eds: S. Patai, Z. Rappoport), Wiley, Chichester, **1989**, vol. 1, pp. 305–370; f) R. J. P. Corriu, J. C. Young, in: *Chem. Org. Silicon Compd.* (Eds: S. Patai, Z. Rappoport), Wiley, Chichester, **1989**, vol. 2, pp. 1241–1288.
- [2] For recent publications on hexacoordinate silicon complexes see for example: a) A. Kämpfe, E. Kroke, J. Wagler, *Eur. J. Inorg. Chem.* **2009**, 1027–1035; b) K. Lippe, D. Gerlach, E. Kroke, J. Wagler, *Organometallics* **2009**, *28*, 621–629; c) G. W. Fester, J. Wagler, E. Brendler, U. Böhme, D. Gerlach, E. Kroke, *J. Am. Chem. Soc.* **2009**, *131*, 6855–6864; d) S. Metz, C. Burschka, R. Tacke, *Chem. Asian J.* **2009**, *4*, 581–586; e) S. Metz, C. Burschka, R. Tacke, *Organometallics* **2009**, *28*, 2311–2317; f) G. González-García, E. Álvarez, Á. Marcos-Fernández, J. A. Gutiérrez, *Inorg. Chem.* **2009**, *48*, 4231–4238; g) I. Kalikhman, E. Kertsus-Banchik, B. Gostevskii, N. Kocher, D. Stalke, D. Kost, *Organometallics* **2009**, *28*, 512–516; h) S. Yakubovich, B. Gostevskii, I. Kalikhman, D. Kost, *Organometallics* **2009**, *28*, 4126–4132.
- [3] a) J. Yang, J. G. Verkade, *J. Organomet. Chem.* **2002**, *651*, 15; b) H. H. Karsch, P. A. Schlüter, M. Reisky, *Eur. J. Inorg. Chem.* **1998**, 433–436; c) C.-W. So, H. W. Roesky, P. M. Gurubasawaraj, R. B. Oswald, M. T. Gamer, P. G. Jones, S. Blaurock, *J. Am. Chem. Soc.* **2007**, *129*, 12049–12054; d) H. H. Karsch, R. Richter, E. Witt, *J. Organomet. Chem.* **1996**, *521*, 185.
- [4] a) G. W. Fester, J. Wagler, E. Brendler, U. Böhme, G. Roewer, E. Kroke, *Chem. Eur. J.* **2008**, *14*, 3164–3176; b) J. Wagler, U. Böhme, E. Brendler, S. Blaurock, G. Roewer, *Z. Anorg. Allg. Chem.* **2005**, *631*, 2907–2913.
- [5] a) D. Gerlach, E. Brendler, T. Heine, J. Wagler, *Organometallics* **2007**, *26*, 234–240; b) R. Bertermann, A. Biller, M. Kaupp, M. Penka, O. Seiler, R. Tacke, *Organometallics* **2003**, *22*, 4104–4110.
- [6] a) B. Theis, C. Burschka, R. Tacke, *Chem. Eur. J.* **2008**, *14*, 4618–4639; b) O. Seiler, C. Burschka, T. Fenske, T. Troegel, R. Tacke, *Inorg. Chem.* **2007**, *46*, 5419–5424; c) N. Kano, N. Nakagawa, Y. Shinozaki, T. Kawashima, Y. Sato, Y. Naruse, S. Inagaki, *Organometallics* **2005**, *24*, 2823–2826; d) J. Wagler, U. Böhme, E. Brendler, B. Thomas, S. Goutal, H. Mayr, B. Kempf, G. Ya. Remennikov, G. Roewer, *Inorg. Chim. Acta* **2005**, *358*, 4270–4286.
- [7] a) J. Wagler, A. F. Hill, *Organometallics* **2008**, *27*, 6579–6586; b) J. Wagler, A. F. Hill, *Organometallics* **2007**, *26*, 3630–3632; c) A. R. Bassindale, S. J. Glynn, P. G. Taylor, N. Auner, B. Herrschaft, *J. Organomet. Chem.* **2001**, *619*, 132–140.
- [8] I. Kalikhman, B. Gostevskii, M. Botoshansky, M. Kaftory, C. A. Tessier, M. J. Panzner, W. J. Youngs, D. Kost, *Organometallics* **2006**, *25*, 1252–1258.
- [9] a) J. Herzfeld, A. E. Berger, *J. Chem. Phys.* **1980**, *73*, 6021; b) J. Mason, *Solid State Nucl. Magn. Reson.* **1993**, *2*, 285.
- [10] a) *Calculation of NMR and EPR parameters: Theory and Applications* (Eds.: M. Kaupp, M. Bühl, V. G. Malkin), Wiley-VCH, **2004**; b) A. M. Köster, P. Calaminici, M. E. Casida, R. Flores-Moreno, G. Geudtner, A. Goursot, T. Heine, A. Ipatov, F. Janetzko, J. M. del Campo, S. Patchkovskii, J. Ulises Reveles, D. R. Salahub, A. Vela, *deMon2k* developers, **2006**; c) M. J. Frisch, G. W. Trucks, H. B. Schlegel, G. E. Scuseria, M. A. Robb, J. R. Cheeseman, J. A. Montgomery, Jr., T. Vreven, K. N. Kudin, J. C. Burant, J. M. Millam, S. S. Iyengar, J. Tomasi, V. Barone, B. Mennucci, M. Cossi, G. Scalmani, N. Rega, G. A. Petersson, H. Nakatsuji, M. Hada, M. Ehara, K. Toyota, R. Fukuda, J. Hasegawa, M. Ishida, T. Nakajima, Y. Honda, O. Kitao, H. Nakai, M. Klene, X. Li, J. E. Knox, H. P. Hratchian, J. B. Cross, V. Bakken, C. Adamo, J. Jaramillo, R. Gomperts, R. E. Stratmann, O. Yazyev, A. J. Austin, R. Cammi, C. Pomelli, J. W. Ochterski, P. Y. Ayala, K. Morokuma, G. A. Voth, P. Salvador, J. J. Dannenberg, V. G. Zakrzewski, S. Dapprich, A. D. Daniels, M. C. Strain, O. Farkas, D. K. Malick, A. D. Rabuck, K. Raghavachari, J. B. Foresman, J. V. Ortiz, Q. Cui, A. G. Baboul, S. Clifford, J. Cioslowski, B. B. Stefanov, G. Liu, A. Liashenko, P. Piskorz, I. Komaromi, R. L. Martin, D. J. Fox, T. Keith, M. A. Al-Laham, C. Y. Peng, A. Nanayakkara, M. Challacombe, P. M. W. Gill, B. Johnson, W. Chen, M. W. Wong, C. Gonzalez, J. A. Pople, *Gaussian 03*, Revision C.02, Gaussian, Inc., Wallingford, CT, **2004**; d) G. te Velde, F. M. Bickelhaupt, E. J. Baerends, C. Fonseca Guerra, S. J. A. van Gisbergen, J. G. Snijders, T. Ziegler, *J. Comput. Chem.* **2001**, *22*, 931; e) ADF 2008.01, *ADF User's Guide*, <http://www.scm.com>, SCM, Theoretical Chemistry, Vrije Universiteit, Amsterdam.

Received: August 12, 2009

Published Online: December 8, 2009